ARMA 16-620

Failure criterion with intermediate stress and two friction angles

Labuz, J.F.
Department of Civil, Environmental, and Geo- Engineering, University of Minnesota, Minneapolis, MN, USA
Makhnenko, R.Y.
Laboratory of Soil Mechanics, Swiss Federal Institute of Technology (EPFL), Lausanne, Switzerland
Harvieux, J.T.
Department of Civil and Environmental Engineering, Stanford University, CA, USA

ABSTRACT: For many rock types, Mohr-Coulomb (MC) failure criterion is a reasonable approximation to strength data, featuring a linear relation with two principal stresses and two material parameters that describe a stress intercept (*e.g.* uniaxial compression or uniform triaxial tension) and pressure sensitivity (*e.g.* internal friction angle ϕ). A criticism of MC is the absence of the intermediate principal stress. Paul-Mohr-Coulomb (PMC) criterion removes that limitation by including three principal stresses. PMC has the advantage over other multi-axial stress criteria in that three material constants, such as one stress intercept and two friction angles, one for compression ϕ_c and one for extension ϕ_e, are readily identified.

PMC failure criterion is reviewed and data from a series of conventional triaxial compression and extension experiments on Indiana limestone are analyzed. The extension friction angle is larger than the compression friction angle, a sufficient but not necessary condition of the intermediate stress effect. To capture the behavior of the rock in multi-axial loading, PMC is extended to include the results of plane strain compression experiments through the construction of two planes with six parameters.

1. INTRODUCTION

A failure criterion can always be written as a function of principal stresses $\sigma_I \geq \sigma_{II} \geq \sigma_{III}$ or $\sigma_1, \sigma_2, \sigma_3$ with no regard to magnitude. As proposed by Paul (1968), and in a special form by Haythornthwaite (1962), the simplest failure criterion applicable to rock in the brittle regime is a linear function:

$$A\sigma_I + B\sigma_{II} + C\sigma_{III} = 1 \qquad (1)$$

Meyer and Labuz (2013) named this failure criterion Paul-Mohr-Coulomb (PMC) and wrote it as

$$N_c\sigma_I + (N_e - N_c)\sigma_{II} - (N_e + 1)\sigma_{III} = V_o \qquad (2)$$

where V_o is the theoretical – it is not measured – uniform triaxial (all-around equal) tensile strength and

$$N_c = \left[\frac{1-\sin\phi_c}{2\sin\phi_c}\right],\ N_e = \left[\frac{1-\sin\phi_e}{2\sin\phi_e}\right] \qquad (3)$$

where ϕ_c is the friction angle for compression ($\sigma_{II} = \sigma_{III}$) and ϕ_e is the friction angle for extension ($\sigma_{II} = \sigma_I$). PMC can be evaluated by performing conventional triaxial testing on a right circular cylinder, where axial stress σ_a is applied independent of radial stress σ_r to achieve either compression failure, which involves axial shortening, or extension failure, which involves axial lengthening. Note that Mohr-Coulomb (MC) criterion is recovered when $\phi_c = \phi_e = \phi$ ($N_c = N_e$), with $V_o\sin\phi = S_o\cos\phi$; S_o is the shear stress intercept on a Mohr plane known as cohesion. PMC and MC are approximations to the observed failure response, which exhibits a nonlinear variation of strength with mean stress $P = (\sigma_1+\sigma_2+\sigma_3)/3$, although PMC contains the intermediate principal stress σ_{II}, which for many rock types, influences strength (Paterson and Wong 2005; Mogi 2007; Haimson and Rudnicki 2010; Ingraham *et al.* 2013; Cornet 2015).

This work reviews the use of PMC with axi-symmetric and multi-axial strength data by implementing a plane fitting approach. Conventional triaxial and plane strain tests were performed on Indiana limestone. The results are plotted in principal stress space and material parameters are determined in the context of friction angles ϕ_c and ϕ_e and the uniform triaxial tensile strength V_o, which is the vertex of a six-sided failure surface in principal stress space (Fig. 1). Additionally, using plane strain data, a twelve-sided failure surface with four friction angles and two different vertices is developed.

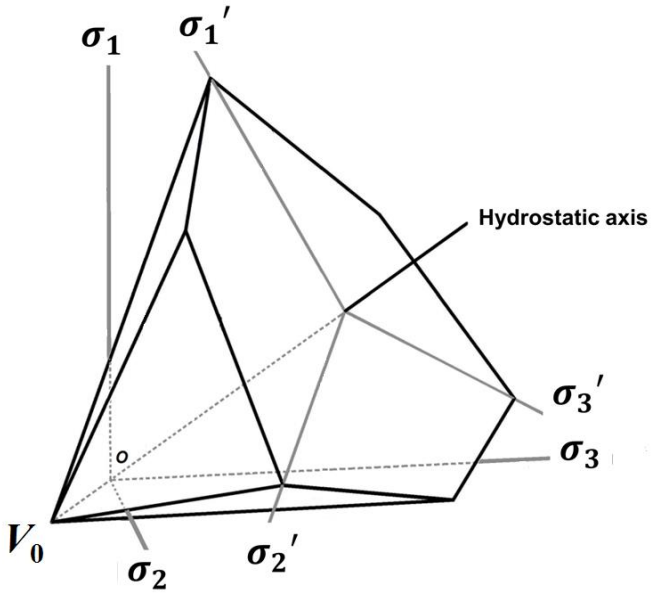

Fig. 1. Linear failure surfaces in principal stress space.

2. BACKGROUND

Isotropic rock exhibits the same (strength) properties in all directions, and thus the orientation of the principal stresses does not matter. Principal stresses can be designated σ_1, σ_2, σ_3 with no regard to magnitude and six orderings appear: (i) $\sigma_1 \geq \sigma_3 \geq \sigma_2$, (ii) $\sigma_3 \geq \sigma_1 \geq \sigma_2$, (iii) $\sigma_3 \geq \sigma_2 \geq \sigma_1$, (iv) $\sigma_2 \geq \sigma_3 \geq \sigma_1$, (v) $\sigma_2 \geq \sigma_1 \geq \sigma_3$, and (vi) $\sigma_1 \geq \sigma_2 \geq \sigma_3$. Therefore, Equation (1) in σ_1, σ_2, σ_3 space gives an irregular hexagonal pyramid because of the six planes for the six orderings of the principal stresses (Fig. 1). Certain features are readily identified: (a) The intersection of the failure surface with the hydrostatic axis ($\sigma_1 = \sigma_2 = \sigma_3$) is V_o, and this point is not measured but it is a basic geometric feature of any pyramidal failure surface. (b) The plane normal to the hydrostatic axis is called the π-plane and the projections of the coordinate axes are labeled σ'_1, σ'_2, σ'_3. (c) With multi-axial testing, *e.g.* plane strain compression, two planes (or more) can be used to fit the data and the failure surface appears as a twelve-sided pyramid with five (four friction angles and the same V_o) or six (four friction angles and two values of V_o) material parameters (Meyer and Labuz 2013).

3. EXPERIMENTAL METHODS

Indiana limestone was used for testing. A single block, 225x215x200 mm (x, y, z-axes), with density ρ = 2300 kg/m^3 and porosity n = 13%, was used to fabricate all specimens. Ultrasonic velocity measurements showed that the rock has a low level of elastic anisotropy, less than 3%. Uniaxial compressive strength (UCS, C_o) tests were performed on four cylindrical specimens, height = 82–90 mm, diameter = 31.5 mm, loaded at an axial displacement rate of 5x10^{-4} mm/s. The UCS = 43–44 MPa, with no directional dependence. Measuring axial and tangential strains by foil strain gages provided Young's modulus E = 26–29 GPa and Poisson's ratio ν = 0.19–0.21. Stearic acid was used to reduce frictional constraint and promote homogeneous deformation for all specimens (Labuz and Bridell 1993).

Conventional triaxial testing involves two principal stresses developed by fluid pressure, and the stress state can be described by $\sigma_1 = \sigma_a$, $\sigma_2 = \sigma_3 = \sigma_r$. Triaxial compression loading $\Delta\sigma_a > 0$ was performed with $\sigma_a = \sigma_1$, σ_r = constant; extension unloading $\Delta\sigma_a < 0$ was performed with $\sigma_a = \sigma_{III}$, σ_r = constant. Ten triaxial tests were conducted on limestone specimens, height = 82–90 mm, diameter = 31.5 mm, at an axial displacement rate of ±5x10^{-4} mm/s, where the plus sign was associated with compression loading and the minus sign with extension unloading. Of the ten triaxial tests, six were performed in compression and four in extension. A typical specimen failed in conventional triaxial compression is shown in Fig. 2a. The failure stress for conventional triaxial extension was determined from the minimum axial stress, which corresponded to the maximum principal stress difference.

A plane strain apparatus (Makhnenko and Labuz 2014) was used to investigate multi-axial failure, where $\sigma_I \neq \sigma_{II} \neq \sigma_{III}$. The plane strain condition was achieved through passive restraint by securing the specimen with a pair of wedges and a flat plate within a biaxial frame (Fig. 3). Using strain gages glued to the frame, the measured deformation of the steel cylinder allows a calculation of the intermediate principal stress within ±0.2 MPa. The minor principal stress σ_{III} was maintained constant and the major principal stress σ_I was increased until failure. Three plane strain compression experiments were conducted at σ_{III} = 0, 5, and 10 MPa. A plane strain specimen tested at σ_{III} = 10 MPa is shown in Figure 2b.

(a) (b)

Fig. 2. Limestone specimens after failure; (a) conventional triaxial compression, (b) plane strain compression.

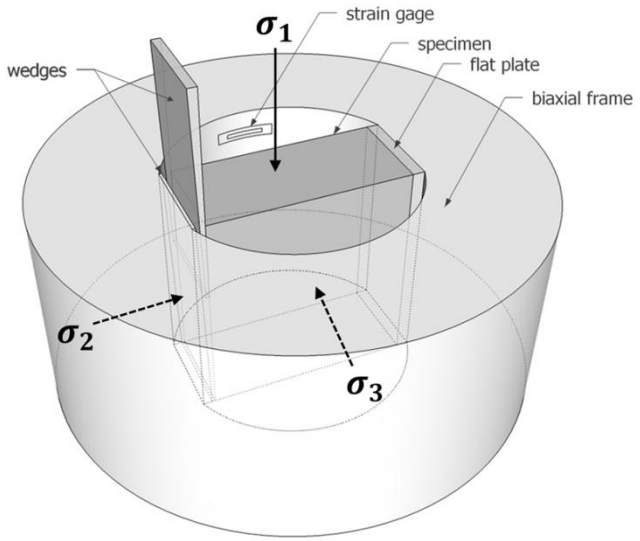

Fig. 3. Plane strain apparatus with prismatic specimen. Plane strain is in the σ_2 direction.

4. RESULTS AND DISCUSSION

The data for all tests is presented in Makhnenko and Labuz (2014). For the axisymmetric stress states, the data are conveniently represented in the *P*-*q* diagram, where $P = (\sigma_a + 2\sigma_r)/3$ and q = deviatoric stress = $\sqrt{3J_2} = (\sigma_a - \sigma_r)$, where J_2 is the second invariant of the deviator stress $S_{ij} = \sigma_{ij} - P\delta_{ij}$. The *P*-*q* plane represents the section of the pyramid from Fig. 1 that contains the hydrostatic and σ'_1 axes, and Equation (1) can be written (Dehler and Labuz 2007), for compression

$$q = \frac{6\sin\phi_c}{3-\sin\phi_c}P + \frac{6c_c\sin\phi_c}{3-\sin\phi_c} \tag{4a}$$

and for extension

$$-q = \frac{6\sin\phi_e}{3+\sin\phi_e}P + \frac{6c_e\sin\phi_e}{3+\sin\phi_e} \tag{4b}$$

In general, the best-fit lines to the compression and extension data in the *P*-*q* plane will not intersect at the same point along the *P*-axis and a constraint in the fitting process must be added. Different friction angles in compression and extension are observed: $\phi_c = 32.1°$, $\phi_e = 35.4°$, and $V_o = 18.5$ MPa (Table 1). The MC surface in the extension region is shown by the broken line in Fig. 4, and it is clear that PMC fits the data better than MC; this rock features a dependence on σ_{II}. Note that $\phi_e > \phi_c$ is a sufficient but not necessary condition of the intermediate stress effect; *i.e.* the friction angles can be equal but failure at other stress states may depend on σ_{II}.

The plane fitting approach of Makhnenko *et al.* (2015) was used to determine the material parameters, and the assumption of isotropy allows the extension data to be moved to the plane of the failure surface containing the compression data. A plane describing the failure surface

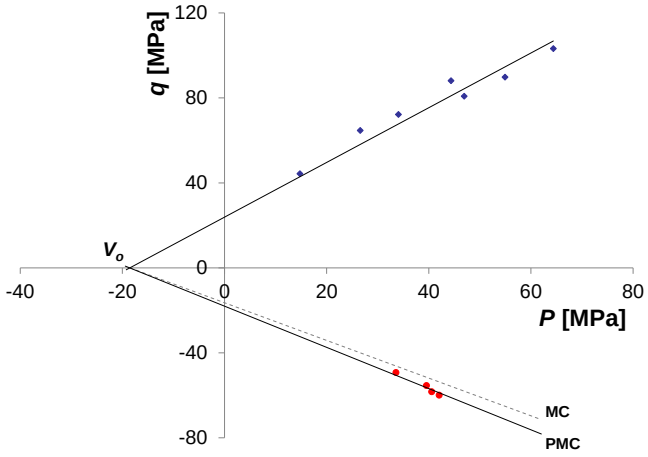

Fig. 4. Results of triaxial tests in *P*-*q* plane.

can then be fitted through a least squares approach that was scaled by the range of the data sets.

The least squares fit involves finding the minimum of the sum of squared orthogonal distances in terms of stress magnitude, between the points and the plane. With the equation of the plane written as $A\sigma_1 + B\sigma_2 + C\sigma_3 = 1$, the sum of squared distances is:

$$\sum \delta_i^2 = \frac{1}{A^2+B^2+C^2}\sum\left(A\sigma_{1,i} + B\sigma_{2,i} + C\sigma_{3,i} - 1\right)^2 \tag{5}$$

where δ_i is the orthogonal stress magnitude between point $i = (\sigma_{1,i}, \sigma_{2,i}, \sigma_{3,i})$ and the plane. A normalization technique with a scaling factor α was used because the compression data spanned a much larger range than the extension data. The normalized plane fitting equation is:

$$\frac{\sum \delta_{j,c}^2}{r_c^2} + \frac{\sum \delta_{k,e}^2}{\alpha r_e^2} = \text{minimum} \tag{6}$$

where $r_{c,e}$ is the maximum range in principal stress space between data points from compression, extension tests ($r_c = 72.7$ MPa, $r_e = 17.0$ MPa). Partial derivatives with respect to *A*, *B*, and *C* were computed, set equal to zero, and the system of equations was solved. V_o was determined by finding the point where the plane intersects the hydrostatic axis ($\sigma_1 = \sigma_2 = \sigma_3$). The other five sides of the six-sided pyramidal failure surface were formed by exchanging the values of *A*, *B*, and *C*. The results of the procedure in terms of V_o, ϕ_c, and ϕ_e are presented in Table 1 and the hexagonal pyramid is shown in Fig. 5. With $\alpha = 1.0$, both line fitting with a constraint and plane fitting give similar results.

To include multi-axial test data from the plane strain experiments ($r_b = 59.3$ MPa), PMC was extended to construct two planes, with the potential to form a twelve-sided pyramid (Fig. 6), where equations of two independent planes were determined. Plane PL 1 fits the

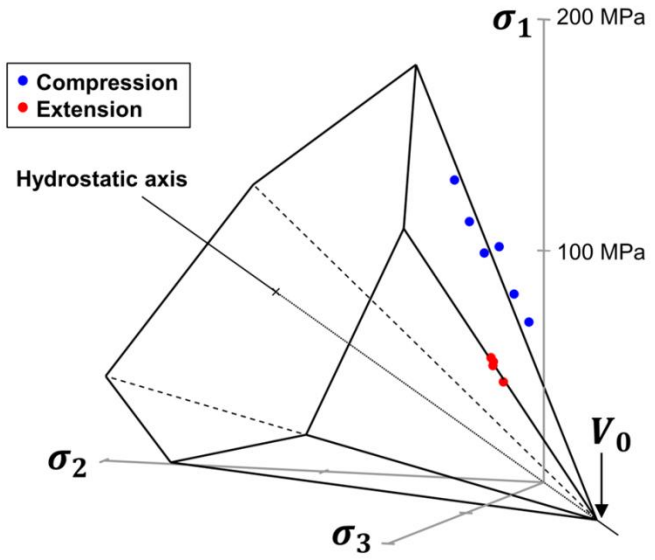

Fig. 5. Six-sided Paul-Mohr-Coulomb (PMC) failure surface fit to Indiana limestone conventional triaxial test data.

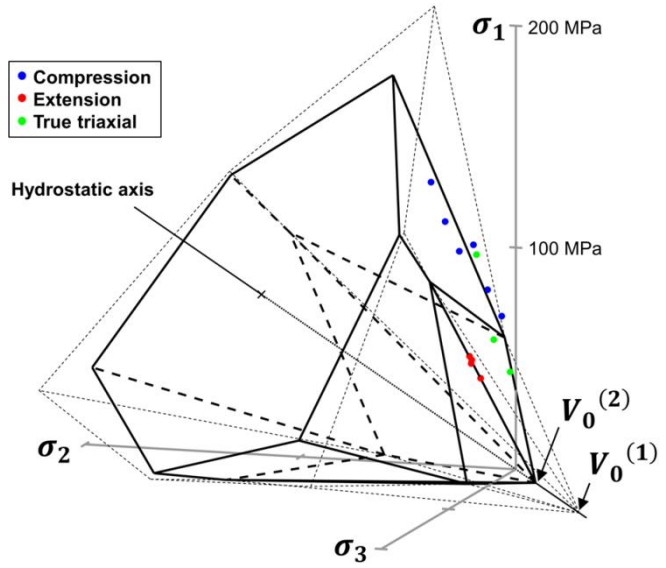

Fig. 6. PMC failure surface featuring two 6-sided pyramids with two different intercepts V_o, giving a 12-sided pyramid over a given region.

data from compression and plane strain tests; PL 2 contains the data for extension and plane strain tests.

The results of the fitting are shown in Fig. 6, in principal stress space, and Fig. 7, in the π-plane. The two fitted planes are each associated with three material parameters ($V_o^{(i)}$, $\phi_c^{(i)}$, $\phi_e^{(i)}$), i = 1, 2 to give a total of six (Table 1). The broken portions of the planes are not realized at every π-plane section, in that the failure response is reached along a particular stress path before the stress state associated with the other portion of the plane.

It is interesting to evaluate the consequences of two values of V_o, which is allowed within the PMC model, and the plane fitting for Indiana limestone displays this feature: (a) Depending on the pressure, the shape in the π-plane changes, as indicated by the three sections in Fig. 7. (b) At a low mean stress, the twelve-sided pyramid switches to six-sided and PL 2 controls failure, as shown in Figs. 6 and 7.

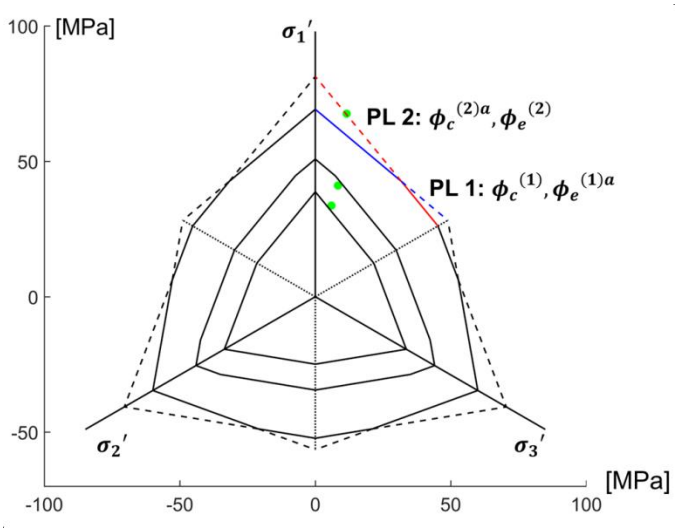

Fig. 7. π-planes of constant mean stress for the plane strain data, with the changing cross-section of the failure surface at three different values of mean stress.

Table 1. Line and plane fitting results for compression, extension, and plane strain data.

Line fitting w/ constraint P-q plane	One plane, normalized least squares, α =1.0	Two planes, normalized least squares, α = 1.0
V_o = 18.5 MPa ϕ_c = 32.1° ϕ_e = 35.4° R_c^2 = 0.926 R_e^2 = 0.926	V_o = 17.8 MPa ϕ_c = 32.5° ϕ_e = 36.0°	PL 1: $V_o^{(1)}$ = 22.5 MPa $\phi_c^{(1)}$ = 31.0° $\phi_e^{(1)}$ = 37.6° PL 2: $V_o^{(2)}$ = 7.0 MPa $\phi_c^{(2)}$ = 46.0° $\phi_e^{(2)}$ = 49.6°

Thus, with two values of V_o, two six-sided pyramids are positioned to form a twelve-sided pyramid over a portion of the region. Outside this region, at both low and high P, a six-sided pyramid (the "inner" one) is the failure surface. The values of P where the switch from six to twelve to six sides occur are determined by the six material parameters.

PMC has this unique feature where the shape of the failure surface in the π-plane changes, and this behavior is often observed for rock. It should be noted that PMC applies for response in the brittle regime displaying shear-type failure. It must be modified when (a) one or more principal stresses are tensile using tension cut-offs (Paul 1961), and (b) the mean stress is large using a "cap" model (DiMaggio and Sandler 1971).

5. SUMMARY

The Paul-Mohr-Coulomb (PMC) failure criterion can be directly applied to conventional triaxial compression and extension data by assuming isotropy and fitting a plane in principal stress space. This results in a six-sided pyramidal failure surface with three material parameters: the (theoretical) uniform triaxial tensile strength, friction angle for compression, and friction angle for extension. For uniaxial tension or large mean stress, this model does not accurately describe behavior, and tension cut-offs and a cap model should be introduced. Nonetheless, PMC failure criterion is a convenient approximation to the complicated nonlinear response in the π-plane, and PMC includes the intermediate stress effect, where the internal friction angle can be larger in extension than compression.

PMC can be extended by including true triaxial test data, and two different planes can be fit to the data, which creates a twelve-sided failure surface, over a portion of the region, from the two intersecting six-sided pyramidal surfaces. A total of six material parameters can be calculated, three corresponding to each fitted plane.

ACKNOWLEDGEMENTS

Partial support was provided by the DOE Grant DE-FE0002020 and the UMN Undergraduate Research Opportunities Program (UROP). J. Meyer assisted with experimental design.

REFERENCES

1. Cornet, F. (2015). *Elements of Crustal Geomechanics*. Cambridge University Press.
2. Dehler, W. and J.F. Labuz (2007). Stress path testing of an anisotropic sandstone. *J. Geotech. Engng. ASCE.* 133: 116-119.
3. DiMaggio, F.L. and I.S. Sandler. 1971. Material model for granular soils. *J. Eng. Mech. Div*. 97: 935-950.
4. Haimson, B. and J.W. Rudnicki. 2010. The effect of the intermediate principal stress on fault formation and fault angle in siltstone. *J. Struct. Geol.* 32: 1701-1711.
5. Haythornthwaite, R.M. 1962. Range of yield condition in ideal plasticity. *Trans. ASCE* 127, Part I: 1252-1267.
6. Ingraham, M.D., K.A. Issen, and D.J. Holcomb. 2013. Response of Castlegate sandstone to true triaxial states of stress. *J. Geophys. Res. Solid Earth* 118: 536-552.
7. Labuz, J.F. and J.M. Bridell. 1993. Reducing frictional constraint in compression testing through lubrication. *Int. J. Rock Mech. Min. Sci. Geomech. Abstr.* 30: 451-455.
8. Makhnenko, R. and J. Labuz. 2014. Plane strain testing with passive restraint. *Rock Mech. Rock Eng.* 47(6): 2021-2029.
9. Makhnenko, R.Y., J. Harvieux, and J.F. Labuz. 2015. Paul-Mohr-Coulomb failure surface of rock in the brittle regime. *Geophys. Res. Lett.* 42: 6975-6981.
10. Meyer, J.P. and J.F. Labuz. 2013. Linear failure criteria with three principal stresses. *Int. J. Rock Mech. Min. Sci.* 60: 180-187.
11. Mogi, K. 2007. *Experimental Rock Mechanics*. London: Taylor & Francis Group.
12. Paterson, M.S. and T.-f. Wong. 2005. *Experimental Rock Deformation – The Brittle Field*. 2nd ed. Berlin: Springer-Verlag.
13. Paul, B. 1961. A modification of the Coulomb-Mohr theory of fracture. *J. Appl. Mech*. 28: 259-268.
14. Paul, B. 1968. Generalized pyramidal fracture and yield criteria. *Int. J. Solids Struct*. 4: 175-196.